Experimental Cell Research **261,** 119–126 (2000)
doi:10.1006/excr.2000.5062, available online at http://www.idealibrary.com on IDEAL®

Apoptosis of Syncytia Induced by the HIV-1–Envelope Glycoprotein Complex: Influence of Cell Shape and Size

Karine F. Ferri, Etienne Jacotot, Philip Leduc,* Maurice Geuskens,† Donald E. Ingber,* and Guido Kroemer[1]

*Centre National de la Recherche Scientifique, UMR1599, Institut Gustave Roussy, 39 rue Camille-Desmoulins, F-94805 Villejuif, France; *Departments of Surgery and Pathology, Children's Hospital and Harvard Medical School, Enders 1007, 300 Longwood Avenue, Boston, Massachusetts 02115; and †Laboratory of Molecular Parasitology, Université Libre de Bruxelles, B-6041 Gosselies, Belgium*

Cells stably transfected with a lymphotropic HIV-1 *Env* gene form syncytia when cocultured with $CD4^+CXCR4^+$ cells. Heterokaryons then spontaneously undergo apoptosis, while manifesting signs of mitochondrial membrane pemeabilization as well as nuclear chromatin condensation. Modulation of cellular geometry was achieved by growing syncytia on self-assembled monolayers of terminally substituted alkanethiolates designed to control the adhesive properties of the substrates. Spreading of syncytia, induced by culturing them on small circular adhesive islets (diameter 5 μm), placed at a distance that cells can bridge (10 μm), inhibited spontaneous and staurosporin-induced signs of apoptosis, both at the mitochondrial and at the nuclear levels, and allowed for the generation of larger syncytia. Transient cell spreading conferred a memory of apoptosis inhibition which was conserved upon adoption of a conventional cell shape. Limiting syncytium size by culturing them on square-shaped planar adhesive islands of defined size (400 to 2500 μm^2), separated by nonadhesive regions, enhanced the rate of apoptotic cell death, as indicated by an accelerated permeabilization of the outer mitochondrial membrane, loss of the mitochondrial inner transmembrane potential, and an increased frequency of nuclear apoptosis. In conclusion, external constraints on syncytial size and shape strongly modulate their propensity to undergo apoptosis. **© 2000 Academic Press**

Key Words: **AIF; cell death; cell geometry; cytochrome *c;* mitochondria.**

INTRODUCTION

Apoptosis may be defined as a form of cell death in which the activation of catabolic hydrolases (caspases and nucleases) contributes to the acquisition of a stereotyped pattern of biochemical and morphological alterations and, in particular, chromatin condensation [1]. In the so-called intrinsic pathway of apoptosis, caspase and nuclease activation relies on mitochondrial membrane permeabilization with loss of the transmembrane potential ($\Delta\Psi_m$)[2] and/or release of proteins from the intermembrane space [2–4]. Cytochrome *c* (Cyt. *c*), which is normally confined to mitochondria, is translocated to the cytosol where it interacts with Apaf-1 and triggers (auto)activation of caspase-9, which in turn sets off the caspase activation cascade [5–7]. Yet another mitochondrial intermembrane protein, apoptosis-inducing factor (AIF), is liberated early during the apoptotic process. AIF translocates to both the cytosol and the nucleus where it can induce a large-scale DNA fragmentation and peripheral chromatin condensation [8, 9]. The cytoplasmic and nuclear events accompanying apoptosis obey similar rules in physiological (homeostatic) cell death and under pathological conditions in which external agents, including viruses, cause excessive cellular demise [1].

One of the several mechanisms accounting for HIV-1-induced lymphodepletion resides in the capacity of the envelope glycoprotein complex (Env) expressed on HIV-1-infected cells to interact with CD4 and a suitable coreceptor (CXCR4 or CCR5) on the surface of noninfected cells, thereby triggering cell fusion. The vast majority of syncytium-inducing HIV-1 variants employ CXCR4 as a coreceptor, and a strong correlation between infection by syncytium-induced HIV-1 variants and $CD4^+$ T cell decline has been established [10–14]. Formation of syncytia is generally followed by cell death, either by apoptosis or by necrosis, depending on the cell types engaged in the process [15–18]. The exact molecular mechanisms linking the formation of syncytia to cell death are elusive. On

[1] To whom correspondence and reprint requests should be addressed at CNRS–UMR1599, Institut Gustave Roussy, Pavillon de Recherche 1, 39 rue Camille-Desmoulins, F-94805 Villejuif, France. Fax: 33-1-42 11 52 44. E-mail: kroemer@infobiogen.fr. or kroemer@igr.fr.

[2] Abbreviations used: AIF, apoptosis-inducing factor; Cyt. *c*, cytochrome *c;* COX, cytochrome *c* oxidase; $\Delta\Psi_m$, mitochondrial transmembrane potential; Env, envelope glycoprotein complex; FITC, fluorescein isothiocyanate; PE, phycoerythrin; SAM, self-assembled monolayer; STS, staurosporin.

0014-4827/00 $35.00
Copyright © 2000 by Academic Press
All rights of reproduction in any form reserved.

theoretical grounds, they may involve receptor-dependent signaling events, an intrinsic death program of fusion-generated heterokaryons (which are nonphysiological, except in myocytes, syncytiotrophoblasts, osteoclasts, and spermatogonia), a metabolic imbalance due to changes in the surface/volume ratio (which would be distorted, especially in large syncytia), or major changes in cellular and cytoskeletal organization. Histopathological examination of lymphoid tissues from HIV-1-infected individuals reveals that giant multinuclear cells can be detected *in situ*, although at a relatively low frequency [19–23], perhaps because their life span is limited and dying cells are rapidly removed by heterophagy [24]. *In vivo*, the tissue architecture must be expected to impose important constraints on the size as well as on the shape of syncytia that are not revealed *ex vivo* or *in vitro*, under ordinary culture conditions.

The present study was designed to unravel possible effects of size or shape on the fate of syncytia. Recently, a convenient method has been developed to pattern the attachment of anchorage-dependent cells to glass coverslips, thereby modulating cellular geometry [25–27]. The method employs self-assembled monolayers (SAMs) of terminally substituted alkanethiolates adsorbed on optically transparent films of gold to control the properties of the substrates. SAMs terminated in methyl groups (which adsorb fibronectin and thus permit adherence of cells) and SAMs terminated in oligoethylene glycol groups (which repel fibronectin and thus resist adherence of cells) are generated by microcontact printing, thus yielding planar adhesive islands of defined size and shape, separated by nonadhesive regions. Using such cell culture substrates, the maximum size of individual cells or syncytia can be controlled at the micrometer scale by varying the adhesion surface. Moreover, spreading of cells can be induced by stamping small adhesive circular islands (diameter 3–5 μm) at a distance that cells can bridge [25–27]. In addition to impinging on the geometry of cells, patterned SAMs profoundly alter basic parameters of cell physiology such as proliferation, differentiation, and apoptosis, regardless of the matrix protein used to mediate adhesion [27–29]. We have used either conventional culture conditions or micropatterned SAMs to modulate mitochondrial and nuclear signs of apoptosis in syncytia induced by HIV-1–Env/CD4 interaction. Our results indicate that limiting syncytium size by external constraint accelerates the death process and that increased spreading suppresses the spontaneous apoptosis of syncytia.

MATERIALS AND METHODS

Cells and culture conditions. HeLa cells stably transfected with a vector containing the *env* gene of HIV-1 LIF (HeLa 243 Env) [30] or *env* from a monotropic HIV-1 isolate (HeLa Ada, gift from M. Alizon, CGM, Paris, France) [31] were cultured in complete culture medium (DMEM supplemented with 2 mM glutamine, 10% FCS, 1 mM pyruvate, 10 mM Hepes, and 100 U/ml penicillin/streptomycin) containing 2 μM methotrexate. HeLa cells transfected with CD4 (HeLa P4; gift from P. Charneau, Pasteur Institute, Paris, France) [32] were selected in medium containing 500 μg/ml G418. Cocultures of different cell types were performed in complete culture medium, in the absence of selecting antibiotics, by adding trypsinized cells to adherent HeLa CD4 or HeLa Env (density 1–1.5 $\times$ 10^3 cells/mm^2) at an approximate 1:1 ratio. Apoptosis was induced by staurosporin (STS; 2 μM; Sigma) or the CD95-specific IgM mAb CH-11 (500 ng/ml; Immunotech, Marseille, France).

Electron microscopy. Cells were fixed for 1 h at 4°C in 2.5% glutaraldehyde in 0.1 M cacodylate buffer (pH 7.4), washed, and fixed again in 2% osmium tetroxide, before embedding in Epon. Electron microscopy was performed with an AEI 6B electron microscope, at 60 kV, on ultrathin sections (60 nm) stained with uranyl acetate and lead citrate.

Preparation of SAMs. Following published protocols [25, 26], an elastomeric stamp with a relief of the predetermined pattern was used to transfer hexadecanethiol (which is compatible with protein absorption) to designated regions of glass coverslips (200 μm thick, Corning) covered with thin films of titanium (1.5 nm) and gold (12 nm at the surface). The slides were then immersed in 2 mM tri(ethylene glycol)-terminated alkanethiol (which resists the absorption of proteins) reacting with the bare regions of gold remaining after the printing process. Coverslips were stored in a nitrogen atmosphere at 4°C in the dark for a maximum of 8 days and were precoated with human fibronectin (25 μg/ml in PBS, pH 7.2, 2 h, RT; Sigma), blocked with bovine serum albumin (10 mg/ml, 20 min, RT; Sigma), and rinsed with complete culture medium immediately before cell attachment.

Fluorescence staining of live cells. Trypsinized HeLa CD4 cells or adherent HeLa Env cells were labeled with either of two membrane permeant fluorochromes for long-term cell labeling, 5-(and-6)-(((4-chloromethyl) benzoyl)amino)tetramethylrhodamine (CellTracker orange), 8-chloromethyl-4,4-difluoro-1,3,5,7-tetramethyl-4-bora- 3*a*,4*a*-diaza-*s*-indacene (CellTracker green; Molecular Probes; 15 μM, 30 min at 37°C in complete medium), and washed extensively before coculture. For the assessment of mitochondrial and nuclear features of apoptosis, cells cultured on a coverslip were stained with 5,5′,6,6′-tetrachloro-1,1′, 3,3′-tetraethylbenzimidazolylcarbocyanine iodide (JC-1, 2 μM, Molecular Probes [33]) and Hoechst 33342 (2 μM, Sigma) for 30 min at 37°C in complete culture medium. The extent of chromatin condensation, as measured with Hoechst 33342, was quantitated in several stages, as described [9].

Immunofluorescence. A rabbit antiserum generated against a mixture of three peptides derived from the mouse AIF aa sequence (aa 151–170, 166–185, and 181–200, coupled to keyhole limpet hemocyanine) (8) was used (diluted 1/0) on paraformaldehyde (4% w/v) and picric acid-fixed (0.19% v/v) cells and revealed with a goat anti-rabbit IgG conjugated to phycoerythrin (PE) (Southern Biotechnology, Birmingham, AL). Cells were counterstained for the detection of Cyt. *c* (mAb 6H2.B4 from PharMingen, revealed by a goat anti-mouse IgG1 fluorescein isothiocyanate (FITC) conjugate; Southern Biotechnology), hsp60 (mAb H4149 from Sigma, revealed by the same anti-mouse IgG1 FITC conjugate), cytochrome *c* oxidase (COX subunit IV, mAb 2038C12 from PharMingen, revealed by a goat anti-mouse IgG2a FITC conjugate), or DNA (Hoechst 33342, 2 μM, 15 min of incubation at RT). Since the frequency of cells showing an intermediate phenotype for AIF or Cyt. *c* localization (mitochondrial versus diffuse) is low (<1% [7, 9] the assignment of cells to either of the two categories (orthotopic versus translocated phenotype for AIF and Cyt. *c*) was rather unambiguous (<10% variation between different experiments and observers).

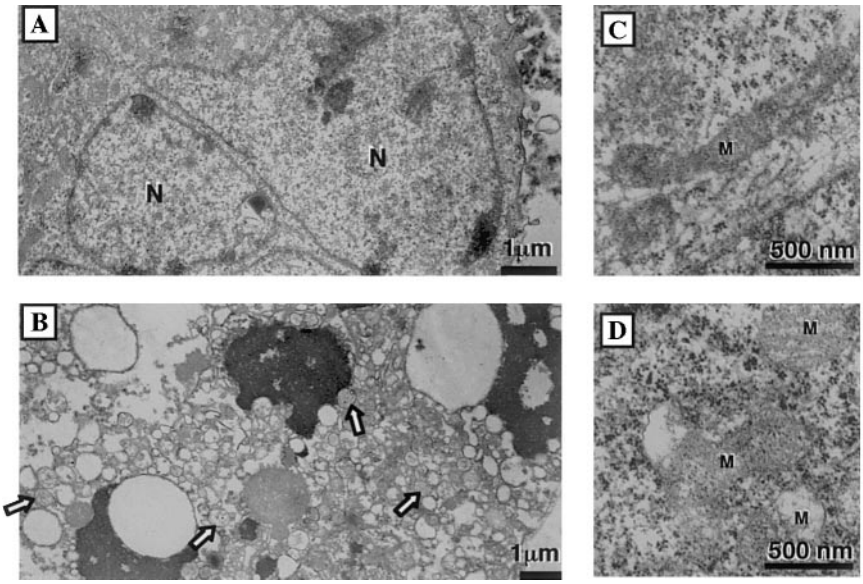

FIG. 1. Ultrastructure of nuclei and mitochondria in syncytia undergoing apoptosis. HeLa Env cells were cultured with HeLa CD4 cells for 24 h (C) or 48 h (A, B, D), respectively. At 48 h, nuclei demonstrate irregular contours with peripheral chromatin condensation (A) or an advanced stage of chromatin condensation (B), paralleling a decrease in mitochondrial matrix (M) density (D, same cell as A) or a strong dilatation of the matrix (arrows in B), when compared to mitochondria from 24-h-old syncytia (C).

RESULTS AND DISCUSSION

Nuclear and mitochondrial signs of apoptosis in syncytia arising from the Env/CD4 interaction. When cocultured on conventional coverslips ("unpatterned substrates"), HeLa cells stably transfected with a lymphotropic HIV-1 *Env* gene (HeLa Env) formed syncytia when cocultured with CD4-expressing HeLa CD4 cells. Twenty-four hours after beginning of cocultures, <25 of syncytia exhibited signs of nuclear apoptosis. This percentage raised to ~50% at 48 h and to ~75% at 72 h (Figs. 1A and 1B). The ultrastructure of mitochondria was characterized by matrix swelling at 48 h of culture in HeLa Env/HeLa CD4 syncytia (Figs. 1B and D), compared to 24 h (Fig. 1C). Matrix swelling was occasionally observed in cells still lacking signs of advanced chromatin condensation (Fig. 1A, same cell as in Fig. 1D). Signs of mitochondrial and nuclear apoptosis could also be monitored by fluorescence light microscopy. Fusion events were monitored by means of stable, nontoxic CellTracker fluorescent dies with which HeLa Env (CellTracker green) or HeLa CD4 cells (CellTracker orange) were preincubated. Syncytium formation was accompanied by blending of the cytoplasmic and nucleoplasmic CellTracker fluorescence, giving rise to a yellow staining (Fig. 2A). Nuclear chromatin condensation was quantitated by staining with Hoechst 33342 (Figs. 2B–2D, blue fluorescence). The apoptosis-associated loss of the mitochondrial transmembrane potential ($\Delta\Psi_m$) was monitored by a spectral shift in the emission wave length of JC-1. Whereas single controls cells possessed a high $\Delta\Psi_m$ (red JC-1 fluorescence), syncytia undergoing apoptosis manifested a low $\Delta\Psi_m$ (green JC-1 fluorescence) (Fig. 2B). *In situ* immunofluorescence was employed to monitor the translocation of AIF (Fig. 2C) or Cyt. *c* (Fig. 2D) from a mitochondrial (see punctate staining in single cells) to an extramitochondrial localization (mainly to the nucleus in the case of AIF, Fig. 2C, and mainly to the cytosol in the case of Cyt. *c,* Fig. 2D) in syncytia. Altogether, the light microscopic examination of HeLa Env/HeLa CD4 syncytia confirms the progressive recruitment of cells into the population with mitochondrial and nuclear signs of apoptosis: ~25, 50, and 75% of the cells, 24, 48, and 72 h after initiation of cocultures on unpatterned control substrates (Fig. 2E).

Spreading of syncytia on micropatterned substrates inhibits apoptosis. Cell fusion may be expected to modify the volume/surface ratio, thereby decreasing the transport or diffusion of essential metabolites or signals. To explore the possibility that a modification in the volume/surface ratio might account for the death of syncytia, we generated HeLa Env/HeLa CD4 heterokaryons on a substrate specifically designed to increase spreading via extension of cell processes that attach to squares of 5 μm in diameter, separated by 10 μm of nonadhesive zones (5/10 SAM) (Fig. 2). This protocol did not reduce syncytia formation (Fig. 2A). The number of nuclei per syncytium actually reached 26 $\pm$ 5 cells after 72 h of coculture, which is significantly higher ($P < 0.01$) than in

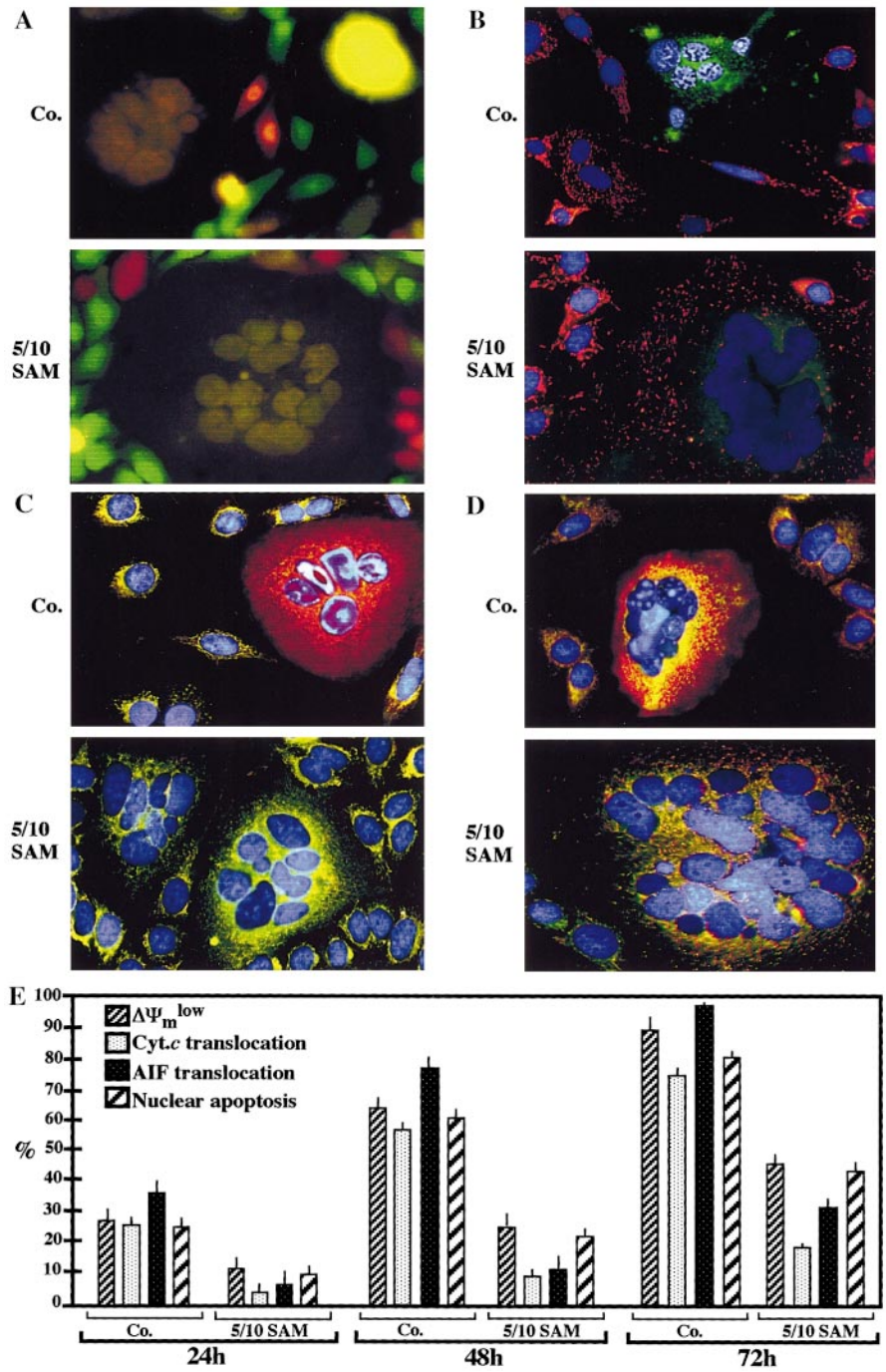

FIG. 2. Mitochondrial and nuclear signs of apoptosis in syncytia cultured on SAMs designed to enhance spreading. Syncytia were either cultured on unpatterned coverslips (Co.) or on SAMs bearing square-shaped adhesive islet of 5 μm in diameter, separated by 10 μm of nonadhesive zones (5/10 SAM). Cells were stained with CytoTracker prior to coculture (A) or at the end of the 72-h incubation period with the $\Delta\Psi_m$-sensitive dye JC-1 (B), an antiserum specific for AIF (revealed by PE, red fluorescence) plus an mAb specific for hsp60 (revealed by FITC, green fluorescence) (C), an mAb specific for Cyt. *c* (revealed by PE) plus an mAb specific for COX (revealed by FITC) (D), and Hoechst 33342 (blue fluorescence in B–D). Note the punctate staining pattern of AIF, Cyt. *c*, hsp60, and COX in single cells serving as intrinsic controls. Due to colocalization of the red and the green fluorescence, mitochondria appear as yellow dots. In apoptotic syncytia, AIF and cytochrome *c* are found in the entire cytoplasm (diffuse red fluorescence). Representative cells are shown. The frequency of apoptosis-associated changes is plotted for different time points in E. Results are pooled from seven experiments yielding similar results. Note that nuclear chromatin condensation occurred simultaneously in all nuclei of the same syncytium. Therefore, the percentage of nuclear apoptosis, as detected with Hoechst 33342, corresponds to the percentage of syncytia that contain condensed nuclei.

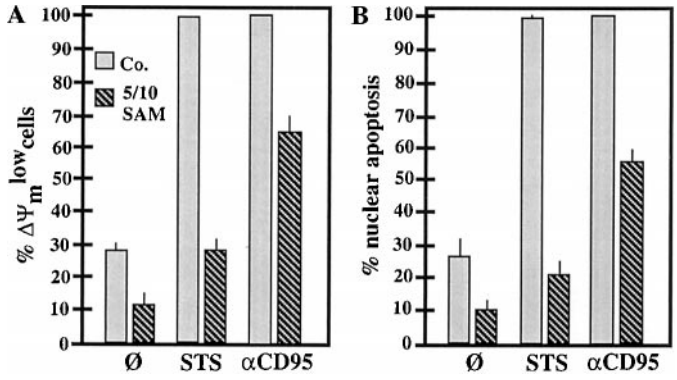

FIG. 3. Apoptosis resistance of cells cultured on control coverslips (Co.) or on 5/10 SAMs. Syncytia were generated by coculture of HeLa Env and HeLa CD4 (24 h) and were then cultured in the absence (Ø) or presence of staurosporin (STS) or a crosslinking anti-CD95 antibody for 2 h, followed by staining with JC-1 and Hoechst 33342. The frequency of cells with a low $\Delta\Psi_m$ (A) or signs of chromatin condensation (B) was then determined. This experiment has been repeated twice, yielding similar results.

controls cultured on a nonpatterned substrate (13 ± 2 nuclei per cell). Concomitantly, nuclear chromatin condensation was blocked by culture on the 5/10 SAM (Figs. 2C and 2D). Mitochondria from most (>90%) syncytia cultured on 5/10 SAM retained AIF (Fig. 2C) and Cyt. *c* (Fig. 2D), and 70–80% of the cells exhibited an intact $\Delta\Psi_m$ (Figs. 2B and 2D). This contrasts with cells cultured on nonpatterned substrates, where most syncytia display signs of nuclear apoptosis (Fig. 2A) and mitochondrial membrane permeabilization (Figs. 2B–2D). As a result, modifications of the cellular architecture by culture on 5/10 SAM can inhibit the mitochondrial alterations accompanying apoptosis, prevent chromatin condensation, and allow for the generation of larger syncytia.

Memory of apoptosis inhibition by enforced spreading. When stimulated with the general apoptosis inducer STS, syncytia cultured on 5/10 SAM exhibited a lower level of $\Delta\Psi_m$ loss (Fig. 3A) and a strongly reduced index of chromatin condensation compared to controls kept on a nonpatterned substrate (Fig. 3B). Similar results were obtained when apoptosis was induced with the topoisomerase II inhibitor etoposide (not shown) or by crosslinking of CD95 (Figs. 3A and 3B). Cytoprotection conferred by 5/10 SAM may involve a change in the volume/surface ratio and/or changes in cytoskeletal organization affecting signal transduction and/or alter the balance of apoptosis regulatory molecules in an active fashion. To investigate this latter possibility, syncytia cultured on a 5/10 SAM were detached from the substrate by trypsinization and reattached to a nonpatterned surface, on which they adopted a morphology that is indistinguishable from that of control syncytia cultured on a nonpatterned substrate throughout the experiment. Nonetheless, those syncytia that had been precultured on a 5/10 SAM retained a relative resistance to staurosporin-induced $\Delta\Psi_m$ dissipation (Fig. 4A) and nuclear apoptosis (Fig. 4B). In conclusion, transient cell spreading on a 5/10 SAM confers a "memory" of anti-death activity which is conserved upon adoption of a classical cell shape.

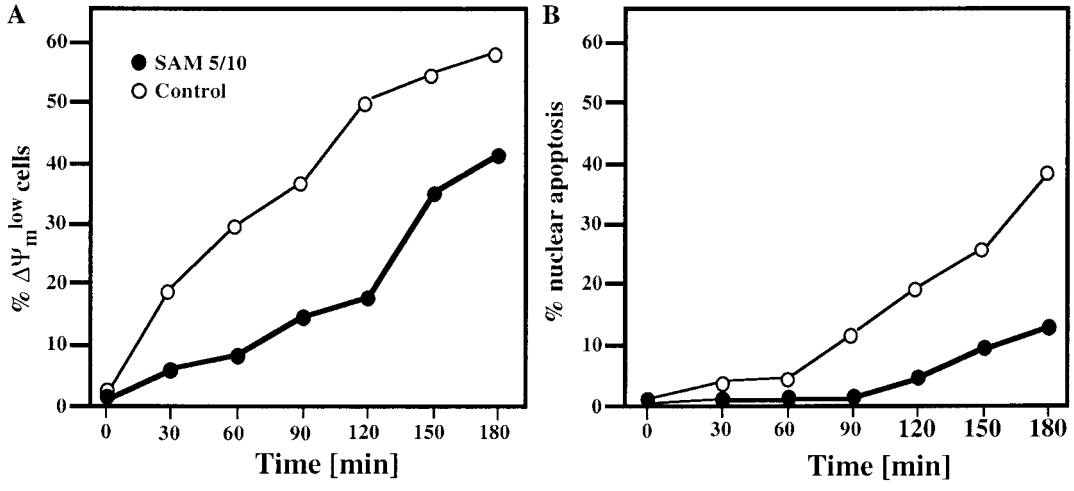

FIG. 4. Apoptosis resistance mediated by transient spreading on 5/10 SAMs. HeLa Env/CD4 syncytia were cultured either on control coverslips (Co.) or on 5/10 SAMs for 18 h and then detached by trypsinization (which does not cause lysis of syncytia), washed, and allowed to readhere to control coverslips, with a surface area 10 greater than that from which cells had been detached. The resulting reduction in cell density largely prevents neoformation of syncytia. After 12 h of culture, syncytia were then exposed to 1 μM STS and the frequency of syncytia exhibiting a low $\Delta\Psi_m$ (A) or nuclear apoptosis (B) was determined at different time points. This experiment has been reproduced three times.

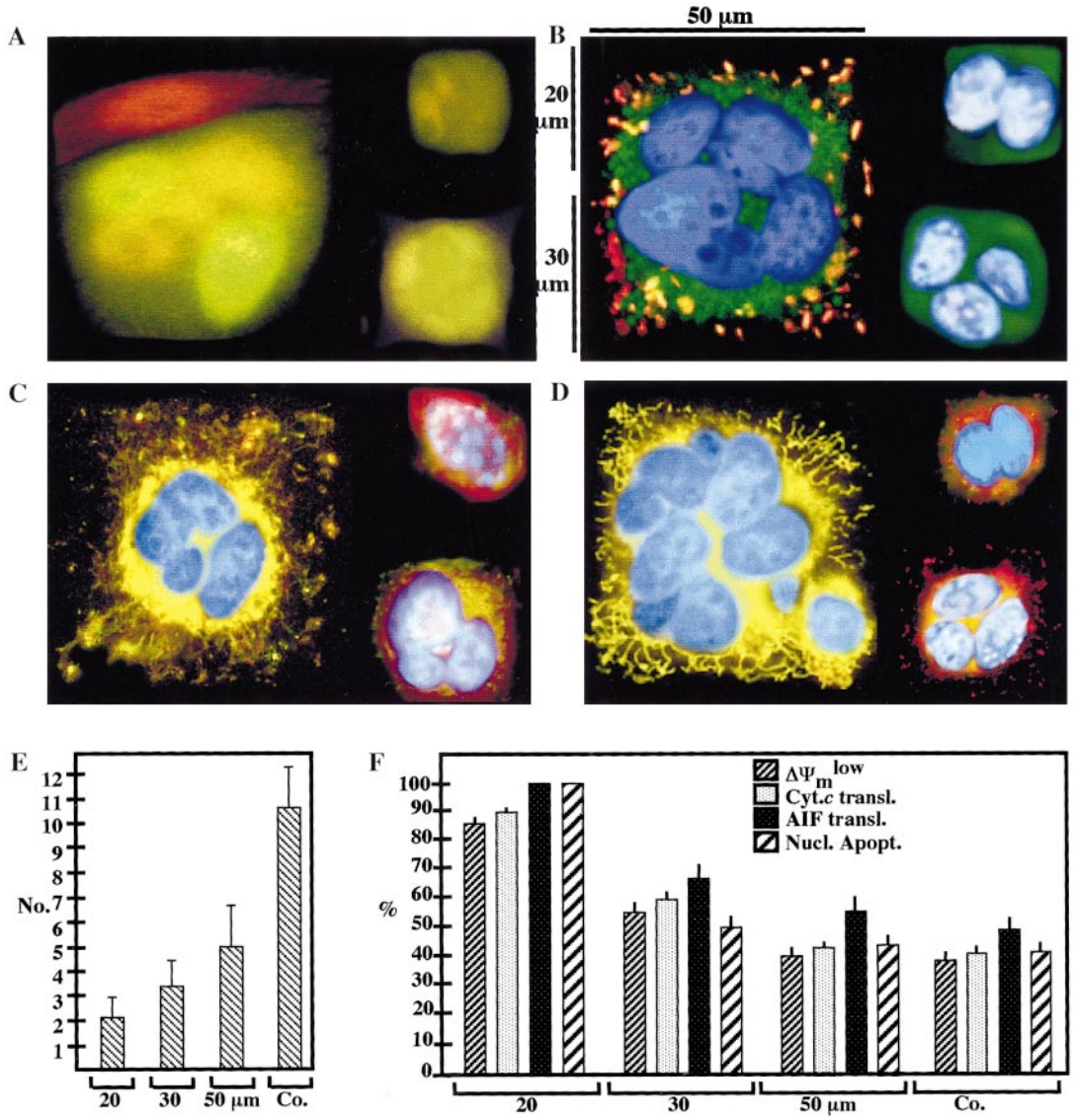

FIG. 5. Mitochondrial and nuclear signs of apoptosis in syncytia cultured on SAMs designed to limit their size. HeLa Env cells were cocultured with HeLa CD4 cells on square-shaped SAMs coated with fibronectin. The experimental readout was based on CytoTracker staining (A), JC-1 staining (B), staining for AIF and hsp60 (C), or staining for Cyt. *c* and COX (D) as in Fig. 4 (staining after 36 h of coculture). Note the diffuse cytosolic staining patterns for AIF and cytochrome *c* obtained in SAMs with dimensions of $\leq$30 μm. Note also the translocation of AIF into the nucleus (purple fluorescence of nuclei in C). The mean number of nuclei per syncytium was determined (E), and the frequency of apoptosis-associated alterations was quantified (F). Results are representative of five independent determinations.

External constraint on syncytial size accelerates apoptosis. In vivo, it may be expected that syncytium formation is limited by the probability of heterologous molecular interactions and/or by adjacent cells not participating in the fusion process. To obtain such a constraint on syncytium size, HeLa Env cells were cocultured with HeLa CD4 cells on square shaped SAMs coated with fibronectin [25–27] (Fig. 5), leading to the generation of square-shaped syncytia. This technique limited the number of nuclei per syncytium (e.g., 4.9 $\pm$ 1.6 on islands of 2500 μm^2, Fig. 5E at 48 h) compared to 10.5 $\pm$ 1.8 on nonpatterned culture substrates ($P < 0.01$). A major a constraint on syncytium size ($\leq$400 μm^2) accelerated chromatin condensation (Figs. 5B–5D) and all mitochondrial signs of apoptosis including $\Delta\Psi_m$ dissipation (Fig. 5B), AIF redistribution to the nucleus (Fig. 5C), and Cyt. *c* translocation to the cytosol (Fig. 5D). Of note, nuclear apoptosis was only found in cells that exhibited signs of mitochondrial membrane permeabilization (Figs. 5B–6D) and a fraction of cells demonstrated Cyt. *c*/AIF translocation before chromatin condensation occurred (Fig. 5F). In conclusion, Env-induced syncytia undergo accelerated apoptosis when their expansion is limited by external constraint.

CONCLUDING REMARKS

The present results are compatible with the hypothesis that external constraints on size and/or shape of syncytia induced via HIV-1–Env/CD4 interaction have a major impact on the intrinsic programmation of syncytia to enter apoptosis. In addition, they provide some mechanistic insights. Signs of mitochondrial membrane permeabilization exhibit a strong correlation with subsequent nuclear apoptosis. $\Delta\Psi_m$ loss (indicative of a permeabilization of the inner membrane) and redistribution of Cyt. *c* or AIF to an extramitochondrial localization (via the outer mitochondrial membrane) occur before chromatin condensation becomes detectable, in syncytia (Figs. 2 and 3). Manipulations which prevent the release of Cyt. *c* and AIF, such as culture of syncytia on the 5/10 SAM, result in an inhibition of nuclear apoptosis (Figs. 2 and 3), thus underscoring the likely cause effect relationship between mitochondrial alterations and nuclear condensation [2–4, 34].

Considering that a syncytium-specific alteration in cellular organization (e.g., a decrease of the surface/volume ratio) could trigger apoptosis by metabolic perturbation and/or imbalances in the reception/processing of signals, we also explored the impact of artificial, support-induced spreading on syncytium apoptosis. Spreading on 5/10 SAMs led to a strongly significant suppression of spontaneous death in syncytia (Fig. 2). However, this death inhibitory effect cannot be attributed to the mere manipulation of the surface/volume ratio, based on two observations. First, spreading reduces apoptosis induction by external signals (staurosporin, crosslinking of CD95), in syncytia as well as individual cells with a normal surface/volume ratio (Fig. 3). Second, even when spread cells have been detached from the culture support and have adopted a nonspread phenotype, they remain relatively resistant to apoptosis induction (Fig. 4), indicating that they conserve a "memory" of death inhibition. This latter observation indicates that, via a hitherto elusive mechanism, transient spreading has led to the persistent accumulation of antiapoptotic regulators (or the durable depletion/inactivation of a death-sensitizing molecule). Thus, spreading does not inhibit apoptosis via an acute signaling event, suggested to involve focal adhesion complex-mediated cell matrix contacts [28, 35], but rather through a persistent change in apoptosis regulation.

Our results provide a clear demonstration that the overall cellular geometry determines the ultimate fate of HeLa Env/HeLa CD4 syncytia. Limiting syncytium size by external constraint, namely by culturing cells on adhesion competent islets of defined size and shape, accelerates the death process (Fig. 5). Syncytia manifest apoptosis as soon as they are limited to a surface $\leq 400\ \mu m^2$ and they contain a maximum of three nuclei (versus a mean of approximately 10 on nonpatterned substrates). It is tempting to speculate that constraints on cell size also apply *in vivo*, in intact tissues, thereby limiting the size of syncytia and accelerating their demise. Cellular geometry manipulated by micropatterned substrates has been shown to affect the expression of genes relevant to cell cycle regulation for extended times, via an effect on the cytoskeleton [29, 36]. It remains elusive how this relates to cell death control. Irrespective of the detailed molecular mechanisms, it appears clear, however, that cellular geometry has a major impact on syncytial apoptosis regulation.

We are indebted to Dr. Dominique Piatier-Tonneau for constant support and to Drs. Marc Alizon and Pierre Charneau for the gift of cell lines. This study was supported by a special grant by the Ligue Nationale contre le Cancer, as well as by grants from ANRS, FRM, the European Commission (to G.K), and NIH (Grant RO1 HL57669-02 to D.E.I.). K.F.F. received a fellowship from the French Ministry of Science; E.J. received an ANRS fellowship. M.G. is a senior research associate of the Belgian National Fund for Scientific Research.

REFERENCES

1. Thompson, C. B. (1995). Distinct roles for the costimulatory ligands B7-1 and B7-2 in T helper cell differentiation? *Cell* **81,** 979–982.
2. Kroemer, G., Dallaporta, B., and Resche-Rigon, M. (1998). The mitochondrial death/life regulator in apoptosis and necrosis. *Annu. Rev. Physiol.* **60,** 619–642.
3. Green, D. R., and Reed, J. C. (1998). Mitochondria and apoptosis. *Science* **281,** 1309–1312.
4. Kroemer, G., and Reed, J. C. (2000). Mitochondrial control of cell death. *Nature Med.* **6,** 513–519.
5. Zhou, H., Henzel, W. J., Liu, X., Lutschg, A., and Wang, X. D. (1997). Apaf-1, a human protein homologous to *C. elegans* Ced-4, participates in cytochrome c-dependent activation of caspase-3. *Cell* **90,** 405–413.
6. Budijardjo, I., Oliver, H., Lutter, M., Luo, X., and Wang, X. (1999). Biochemical pathways of caspase activation during apoptosis. *Annu. Rev. Cell Dev. Biol.* **15,** 269–290.
7. Goldstein, J. C., Waterhouse, N. J., Juin, P., Evan, G. I., and Green, D. R. (2000). The coordinate release of cytochrome c is rapid, complete and kinetically invariant. *Nature Cell Biol.* **2,** 156–162.
8. Susin, S. A., Lorenzo, H. K., Zamzami, N., Marzo, I., Snow, B. E., Brothers, G. M., Mangion, J., Jacotot, E., Costantini, P., Loeffler, M., Larochette, N., Goodlett, D. R., Aebersold, R., Siderovski, D. P., Penninger, J. M., and Kroemer, G. (1999). Molecular characterization of mitochondrial apoptosis-inducing factor. *Nature* **397,** 441–446.
9. Daugas, E., Susin, S. A., Zamzami, N., Ferri, K., Irinopoulos, T., Larochette, N., Prevost, M. C., Leber, B., Andrews, D., Penninger, J., and Kroemer, G. (2000). Mitochondrio-nuclear redistribution of AIF in apoptosis and necrosis. *FASEB J.* **14,** 729–739.
10. Sodroski, J. G., Goh, W. C., Rosen, A., Campbell, K., and Haseltine, W. A. (1986). Role of the HTLV/LAV envelope in syncytia formation and cytopathicity. *Nature* **322,** 470–474.

11. Lifson, J. D., Reyes, G. R., McGrath, M. S., Stein, B. S., and Engleman, E. G. (1986). AIDS retrovirus-induced cytopathology: Giant cell formation and involvement of CD4 antigen. *Science* **232,** 1123–1127.
12. Sylwester, A., Murphy, S., Shutt, D., and Soll, D. R. (1997). HIV-induced T cell syncytia are self-perpetuating ant the primary cause of T cell death in culture. *J. Immunol.* **158,** 3996–4007.
13. Koot, M., Van Leeuwen, R., de Goede, R. E. V., Keet, I. P. M., Danner, S., Schattenkerk, J. K. M. E., Reiss, P., Tersmette, M., Lange, J. M. A., and Schuitemaker, H. (1999). Conversion rate of syncytium-inducing (SI) phenotype during different stages of human immunodeficiency virus type 1 infection and prognostic value of S1 phenotype for survival after AIDS diagnosis. *J. Infect. Dis.* **179,** 254–258.
14. Blaak, H., van't Wout, A. B., Brouwer, M., Hoolbrink, B., Hovenkamp, E., and Schuitemaker, H. (2000). In vivo HIV-1 infection of CD45RA+ CD4+ T cells is established primarily by syncytium-inducing variants and correlates with the rate of CD4+ T cell decline. *Proc. Natl. Acad. Sci. USA* **97,** 1269–1274.
15. Laurent Crawford, A. G., Krust, B., Riviere, Y., Desgranges, C., Muller, S., Kieny, M. P., Dauguet, C., and Hovanessian, A. G. (1993). Membrane expression of HIV envelope glycoproteins triggers apoptosis in CD4 cells. *AIDS Res. Hum. Retroviruses* **9,** 761–773.
16. Sandstrom, P. A., Pardi, D., Goldsmith, C. S., Duan, C. Y., Diamond, A. M., and Folks, T. M. (1996). Bcl-2 expression facilitates human immunodeficiency virus type 1-mediated cytopathic effects during acute spreading infections. *J. Virol.* **70,** 4617–4622.
17. Kolesnitchenko, V., King, L., Riva, A., Tani, V., Korsmeyer, S. J., and Cohen, D. I. (1997). A major human immunodeficiency virus type 1-initiated killing pathway distinct from apoptosis. *J. Virol.* **71,** 9753–9763.
18. Plymale, D. R., Tang, D. S. N., Comardelle, A. M., Fermin, C. D., Lewis, D. E., and Garry, R. G. (1999). Both necrosis and apoptosis contribute to HIV-1-induced kiling of CD4 cells. *AIDS* **13,** 1827–1839.
19. Sharer, L. R., Cho, E.-S., and Epstein, L. G. (1986). Multinucleated giant cells ant HTLV-II in AIDS encephalopathy. *Hum. Pathol.* **16,** 760–765.
20. Witzleben, C. L., Marshall, G. S., Wenner, W., Piccoli, D. A., and Barbour, S. D. (1988). HIV as a cause of giant cell hepatitis. *Hum. Pathol.* **19,** 603–605.
21. Piacentini, M. (1995). "Tissue" transglutaminase as a candidate effector molecule of physiological cell death. *Curr. Top. Microbiol. Immunol.* **200,** 163–176.
22. Amendola, A., Gougeon, M. L., Poccia, F., Bondurand, A., Fesus, L., and Piacentini, M. (1996). Induction of "tissue" transglutaminase in HIV pathogenesis: Evidence for high rate of apoptosis of CD4+ T lymphocytes and accessory cells in lymphoid tissues. *Proc. Natl. Acad. Sci. USA* **93,** 11057–11062.
23. Orenstein, J. M. (1998). The Warthin–Finkeldey-type giant cell in HIV infection, what is it. *Ultrastruct. Pathol.* **22,** 293–303.
24. Savill, J. (1996). Phagocyte recognition of apoptotic cells. *Biochem. Soc. Trans.* **24,** 1065–1069.
25. Mrksich, M., Chen, C. S., Xia, Y., Dike, L., Ingber, D. E., and Whitesides, G. M. (1996). Controlling cell attachment on contoured surfaces with self-assembled monolayers of alkanethiolates on gold. *Proc. Natl. Acad. Sci. USA* **93,** 10775–10778.
26. Mrksich, M., Dike, L. E., Tien, J., Ingber, D. E., and Whitesides, G. M. (1997). Using microcontact printing to pattern the attachment of mammalian cells to self-assembled monolayers of alkanethiolates on transparent films of gold and silver. *Exp. Cell Res.* **235,** 305–313.
27. Chen, C. S., Mrksich, M., Huang, S., Whitesides, G. M., and Ingber, D. E. (1997). Geometric control of cell life and death. *Science* **276,** 1425–1428.
28. Chicurel, M. E., Chen, C. S., and Ingber, D. E. (1998). Cellular control lies in the balance of forces. *Curr. Opin. Cell Biol.* **10,** 232–239.
29. Huang, S., Chen, C. S., and Ingber, D. E. (1998). Control of cyclin D1, p27Kip1 and cell cycle progression in human capillary endothelial cells by cell shape and cytoskeletal tension. *Mol. Biol. Cell* **9,** 3179–3193.
30. Schwartz, O., Alizon, M., Heard, J. M., and Danos, O. (1994). Impairment of T cell receptor-dependent stimulation in CD4+ lymphocttes after contact with membrane-bound HIV-1 envelope glycoprotein. *Virology* **198,** 360–365.
31. Pleskoff, O., Tréboute, C., Brelot, A., Heveker, N., Seman, M., and Alizon, M. (1997). Identification of a chemokine receptor encoded by human cytomegalovirus as a cofactor for HIV-1 entry. *Science* **276,** 1874–1878.
32. Dragic, T., Charneau, P., Clavel, F., and Alizon, M. (1992). Complementation of murine cells for human immunodeficiency virus envelope/CD4-mediated fusion in human/murine heterokaryons. *J. Virol.* **66,** 4794–4802.
33. Smiley, S. T. (1991). Intracellular heterogeneity in mitochondrial membrane potential revealed by a J-aggregate-forming lipophilic cation JC-1. *Proc. Natl. Acad. Sci. USA* **88,** 3671–3675.
34. Vander Heiden, M. G., and Thompson, C. B. (1999). Bcl-2 proteins: Inhibitors of apoptosis or regulators of mitochondrial homeostasis? *Nature Cell Biol.* **1,** E209–E216.
35. Chicurel, M. E., Singer, R. H., Meyer, C. J., and Ingber, D. E. (1998). Integrin binding and mechanical tension induce movement of mRNA and ribosomes to focal adhesions. *Nature* **392,** 730–733.
36. Singhvi, R., Kumar, A., Lopez, G., Stephanopoulos, G. N., Wang, D. I. C., Whitesides, G. M., and Ingber, D. E. (1994). Engineering cell shape and function. *Science* **264,** 696–698.

Received June 30, 2000
Revised version received September 7, 2000